

Editorial Manager(tm) for Nuclear Medicine Communications
Manuscript Draft

Manuscript Number: NMC-05-680R1

Title: Evaluating the Protective Role of Ischemic Preconditioning in Rat Hearts Using a Stationary Small-Animal SPECT Imager and 99mTc-Glucarate

Article Type: Original Study

Section/Category:

Keywords: small-animal SPECT; heart; ischemic preconditioning; rat; 99mTc-glucarate.

Corresponding Author: Research Associate Professor Zhonglin Liu, M.D.

Corresponding Author's Institution: The University of Arizona

First Author: Zhonglin Liu, MD

Order of Authors: Zhonglin Liu, MD; Harrison H Barrett, PhD; Gail D Stevenson, DVM; Lars R Furenlid, PhD; Koon Yan Pak, PhD; James M Woolfenden, MD

Manuscript Region of Origin: UNITED STATES

Abstract: Objective: To examine the protective role of ischemic preconditioning (IPC) in rat hearts using 99mTc-glucarate (GLA) and a stationary SPECT imager, FastSPECT.

Methods: Twenty-four rats with 30-minute myocardial ischemia and 150-minute reperfusion (IR) were studied as bellows. IPC group (n = 6): underwent IPC (5 cycles of 4-minute ligation of the left coronary artery and reflow) before IR; Control group (n = 7): treated by IR without IPC; SPT group (n = 6): subjected to IPC and an adenosine antagonist, 8-(p-sulfophenyl)-theophylline (SPT); Vehicle group (n = 5): received IPC and SPT carrier vehicle. GLA was intravenously delivered 30 minutes post-reperfusion, and 2-hour dynamic cardiac images were acquired by FastSPECT.

Results: GLA showed "hot-spot" accumulation in the ischemic area-at-risk (IAR) and exhibited lower retention (% 5-minute peak) in the IPC and Vehicle groups (33.8 ± 2.6 vs. 35.7 ± 9.2 , $P > 0.05$) than in the Control and SPT groups (63.1 ± 5.3 vs. 54.8 ± 4.8 , $P > 0.05$). The infarct size (% IAR) was larger in the Control

and SPT groups (48.2 ± 6.3 vs. 41.7 ± 6.3 , $P > 0.05$) than that in the IPC and Vehicle groups (21.0 ± 1.9 vs. 19.1 ± 4.6 , $P > 0.05$). In terms of the ex vivo IAR-to-normal radioactive ratio, there was a statistical difference between the Control and IPC groups (7.4 ± 0.9 vs. 3.0 ± 0.4), as well as the SPT and Vehicle groups (7.4 ± 1.0 vs. 3.4 ± 0.5).

Conclusion: IPC offers cardioprotection and relates with the activation of adenosine receptors in rat hearts. FastSPECT GLA imaging is not only useful in detecting early ischemia-reperfusion injury, but also valuable in evaluating cardioprotection.

**Evaluating the Protective Role of Ischemic Preconditioning in Rat Hearts Using a
Stationary Small-Animal SPECT Imager and ^{99m}Tc -Glucarate**

Zhonglin Liu^a, Harrison H. Barrett^a, Gail D. Stevenson^a, Lars R. Furenlid^a, Koon Yan
Pak^b, and James M. Woolfenden^a

^aDepartment of Radiology, University of Arizona, Tucson, AZ, USA

^bMolecular Targeting Technologies, Inc., West Chester, PA, USA

Running head: ^{99m}Tc -glucarate SPECT imaging of rat hearts with IPC

This work was supported by NIH grant P41 EB002035.

For correspondence or reprints contact:

Zhonglin Liu, M.D.

Department of Radiology

The University of Arizona

P. O. Box 245067

Tucson, AZ 85724-5067

Tel. 520-626-4248; Fax. 520-626-2892

E-mail: zliu@radiology.arizona.edu

Abstract

Objective: To examine the protective role of ischemic preconditioning (IPC) in rat hearts using ^{99m}Tc -glucarate (GLA) and a stationary SPECT imager, FastSPECT.

Methods: Twenty-four rats with 30-minute myocardial ischemia and 150-minute reperfusion (IR) were studied as bellows. IPC group (n = 6): underwent IPC (5 cycles of 4-minute ligation of the left coronary artery and reflow) before IR; Control group (n = 7): treated by IR without IPC; SPT group (n = 6): subjected to IPC and an adenosine antagonist, 8-(p-sulfophenyl)-theophylline (SPT); Vehicle group (n = 5): received IPC and SPT carrier vehicle. GLA was intravenously delivered 30 minutes post-reperfusion, and 2-hour dynamic cardiac images were acquired by FastSPECT.

Results: GLA showed “hot-spot” accumulation in the ischemic area-at-risk (IAR) and exhibited lower retention (% 5-minute peak) in the IPC and Vehicle groups (33.8 ± 2.6 vs. 35.7 ± 9.2 , $P > 0.05$) than in the Control and SPT groups (63.1 ± 5.3 vs. 54.8 ± 4.8 , $P > 0.05$). The infarct size (% IAR) was larger in the Control and SPT groups (48.2 ± 6.3 vs. 41.7 ± 6.3 , $P > 0.05$) than that in the IPC and Vehicle groups (21.0 ± 1.9 vs. 19.1 ± 4.6 , $P > 0.05$). In terms of the *ex vivo* IAR-to-normal radioactive ratio, there was a statistical difference between the Control and IPC groups (7.4 ± 0.9 vs. 3.0 ± 0.4), as well as the SPT and Vehicle groups (7.4 ± 1.0 vs. 3.4 ± 0.5).

Conclusion: IPC offers cardioprotection and relates with the activation of adenosine receptors in rat hearts. FastSPECT GLA imaging is not only useful in detecting early ischemia-reperfusion injury, but also valuable in evaluating cardioprotection.

Key Words: Small-animal SPECT; heart; ischemic preconditioning; rat; ^{99m}Tc -glucarate.

Introduction

Small animals, such as rats or mice, can provide models of human cardiovascular disease. Using noninvasive molecular imaging techniques, the small-animal heart models have become valuable tools in the cardiovascular sciences. A high-resolution single-photon emission computed tomography (SPECT) imager, called microSPECT or small-animal SPECT, plays an important role in basic cardiovascular molecular imaging. Because of the small size and fast beating of the heart, high spatial resolution is critical in imaging rat or mouse heart models. Relative to PET, small-animal SPECT has potential advantages in spatial resolution. Currently, several small-animal SPECT systems, either adapted commercial clinical SPECT imagers or specifically designed small-animal SPECT imagers, have been used effectively to image rat hearts and collect validated data of myocardial perfusion, necrosis, and apoptosis with ^{99m}Tc -labeled tracers [1-3]. Modern molecular imaging studies often require investigation of washout rates and other kinetic parameters of radiolabeled agents [4, 5]. The temporal resolution of a small-animal SPECT imager must be high in order to extract accurate estimates of these parameters. Sensitivity is another critical factor in small-animal imaging for acquiring enough photons for good 3-D reconstruction within short periods of time, such as a fraction of a heartbeat or a tracer washout time. Accordingly, a stationary SPECT imager with many cameras has a number of unique advantages over other small-animal SPECT systems, such as the high speed, sensitivity, and resolution plus a stationary gantry. FastSPECT, a standard high-resolution SPECT system built at the University of Arizona, is the first stationary SPECT imager in the world and is capable of producing fast tomographic

images in rats and mice. The acquisition of tomographic data sets in FastSPECT can be executed with no rotation in either animal or detector for dynamic imaging studies.

Using FastSPECT and well-established rat heart models, we previously explored the property of ^{99m}Tc -labeled glucarate (GLA), a novel infarct avid imaging agent, to identify early myocardial ischemia-reperfusion injury. The data from our laboratory and others have demonstrated that ^{99m}Tc -glucarate can mark nonviable regions by hot-spot imaging in myocardium with acute necroses [1, 6-11]. Our experimental studies showed that the severity of myocardial injury induced by different durations of ischemia following reperfusion in the rat heart models can be assessed using GLA noninvasively and quantitatively. From the imaging point of view, investigators and clinicians need a useful tool, not only for identifying varied injuries and status of the heart disease, but also for determining individualized therapeutic strategies and monitoring the effects of therapeutic interventions.

Ischemic preconditioning (IPC) is a process by which exposure of myocardium to a short period of non damaging ischemic stress leads to resistance to the deleterious effects of subsequent prolonged ischemic stress [12]. IPC reduces myocardial infarct size [12-14], improves post-ischemic contractile function [15], and preserves metabolic or energy status of the ischemic-reperfused myocardium [16]. In rat hearts, it is generally believed that adenosine is a trigger for IPC, as it has been well described in other species [15, 17]. However, the exact role and fashion of adenosine in rat hearts with IPC are dissimilar to

the experimental results in other animal hearts [18-20]. Typically, a single cycle of short IPC is insufficient to produce adenosine-mediated cardioprotection; the threshold for producing IPC in rat hearts is higher than in other species. A longer duration stimulus or multiple cycles of short occlusion and reperfusion of the coronary artery are often required to trigger the adenosine receptors. Because the *in vivo* rat heart model with regional ischemia-reperfusion has been used in our laboratory to explore strategies of cardioprotection, we set out to clarify whether or not the adenosine A₁ receptor is involved in an IPC protocol with 5 cycles of 4 minutes of coronary artery occlusion, each separated by 4 minutes of reperfusion for cardioprotection in rat hearts. If adenosine is involved in the specific preconditioning protocol, the nonselective adenosine receptor antagonist, 8-(p-sulphophenyl)-theophylline, SPT, should block the IPC cardioprotection and change the kinetic appearance of GLA in the rat hearts.

Consequently, the objective of this study was to determine if dynamic FastSPECT imaging with GLA would provide a unique, noninvasive tool for evaluation of cardioprotection. We examined the protective role of IPC in ischemic-reperfused rat hearts both noninvasively and quantitatively.

METHODS

Ischemic-Reperfused Rat Heart Model Preparation

Male Sprague-Dawley rats (weighing 250-350 grams) were anesthetized with 1.0%-1.5% isoflurane. The model of myocardial ischemia-reperfusion was developed using the

technique described previously [1]. The rat was ventilated using a volume-controlled Inspira Advanced Safety Ventilator (Harvard Apparatus, Holliston, MA) with oxygen. The chest was opened with a left intercostal thoracotomy incision at the 5th intercostal space. A ligature was placed around the left coronary artery (LCA) with a small amount of myocardium. The ligature was pulled tight by passing the suture through a polyethylene tubing and clamping it repeatedly for coronary occlusion. Regional myocardial reperfusion was elicited by releasing the ligature. After ischemia-reperfusion treatment, the chest of the rat was closed. During the period of surgery, ischemia-reperfusion treatment, and imaging, the body temperature of the animal was maintained with a recirculating warm water pad.

Experimental Protocols and Groups

Group I (IPC, n = 6): animals were preconditioned with a sequence of 5 cycles of 4-minute LCA occlusion and 4-minute reflow; 10 minutes later, the rats underwent a treatment of 30-minute regional myocardial ischemia and 150-minute reperfusion (IR) by ligating and releasing the LCA.

Group II (Control, n = 7): animals received no IPC, but were subjected to equivalent open-chest time as in Group I, then underwent the IR treatment as in Group I.

Group III (SPT, n = 6): rats were subjected to IPC and IR as in Group I. A dose of 8-(p-sulfophenyl)-theophylline (SPT, 10 mg/kg) was infused intravenously 2 minutes before and during subsequent 30-minute ischemia, and then the second dose of SPT was given

within 30-minute reperfusion using a Harvard PHD2000 syringe pump (Harvard Apparatus, Holliston, MA).

Group IV (Vehicle, n = 5): rats were treated with IPC as in Groups I and III followed by IR. Equivalent volume of SPT carrier vehicle (DMSO/saline) was infused intravenously 2 minutes before and during 30-minute ischemia and again within 30-minute reperfusion as in Group III.

Thirty minutes post-reperfusion, GLA was intravenously administered for 120-minute dynamic cardiac FastSPECT imaging in all rats.

Reagents

Glucarate kits were provided by Molecular Targeting Technologies, Inc. (West Chester, PA). A vial of glucarate was reconstituted by the addition of 1.0 ml of ^{99m}Tc as sodium pertechnetate (40 mCi, 1.48 GBq). GLA radiochemical purity (RCP) was verified by thin-layer chromatography using Gelman instant thin-layer silica gel (ITLC-SG) strips developed in saline and acetone. The RCP of GLA exceeded 95% for all experimental injections.

SPT was obtained from Sigma (St. Louis, MO). A stock solution of SPT was prepared in DMSO and diluted with saline for intravenous administration. The dose and administration schedules were applied according to the methods previously described in the literature and our pilot studies [21-23].

Dynamic High-Resolution SPECT Imaging

The small-animal SPECT system, FastSPECT, was built in the Radiology Research Laboratory at the University of Arizona based on a stationary SPECT brain imager [24]. The system consists of 24 small modular gamma cameras and a cylindrical aperture with 24 1-mm diameter pinholes, and it has the capability of rapid SPECT acquisition without motion of the detector or aperture.

Before the animal was loaded into the FastSPECT system, the jugular vein was catheterized through a surgical procedure. The rat was placed inside the aperture using a translation stage. The animal was positioned so that the heart localized in the center of the field of view. Thirty minutes post-reperfusion, GLA (185-222 MBq) was injected intravenously via the jugular vein catheter using the Harvard Apparatus syringe pump, followed by a 0.1-ml saline flush. Beginning immediately upon injection, dynamic cardiac images were acquired every minute for the first 10 minutes, followed by 5-minute acquisition every 15 minutes until 120 minutes post-injection. A total of 24 projections were obtained, one from each camera, to generate a data set for tomographic reconstruction.

Image Processing

Tomographic reconstructions of FastSPECT data were processed using 5 iterations of the algebraic reconstruction technique (ART) algorithm. Three-dimensional images were computed to provide images in a $33 \times 49 \times 49$ -voxel format and to generate tomographic

transaxial, coronal, and sagittal slices with 1-pixel thickness (1.0 mm). The maximum threshold was set at approximately 30-35%, and minimum threshold was set at 0% to display radioactive distribution in the myocardium. The oblique re-orientation of the transaxial data was performed by computerized procedures to generate tomographic short-axis (transverse) slices, which cover the entire left ventricle from the base to the apex. Using AMIDE 0.8.15.1 software, 2-D isocontour regions-of-interest (ROIs) over the “hot-spot” radioactive accumulations were created from all transverse slices on the 120-minute images.

The 120-minute ROIs were applied to all of the dynamic images from 1 to 120 minutes for generating averaged hot-spot time-activity curves (TACs), which were corrected for ROI size (pixels), radioactive decay, acquisition time, and injected dose. The remote normal myocardial time-activity curves were generated using 2-D ROIs analysis. Typically, the left ventricular septum was selected as a remote normal zone to establish the ROI. Care was taken to draw an ROI on the normal zone and avoid the ROI overlapping into the blood pool on the early time-point images. To do that, we used the early blood-pool image to outline the left ventricular wall range. The endocardial edges from tomographic 1-minute cardiac blood-pool images were coregistered with 120-minute images to ensure the ROI establishment off the left ventricular cavity. The percent radioactive retention and washout at each time-point image relative to the initial radioactivity on the 1-minute image and 5-minute image, as well as the ratios of hot-spot activities to remote normal myocardial activities, were calculated subsequently.

Postmortem Analysis

At the end of the imaging session, the LCA was re-occluded. Evans blue dye (10%) in 1.0-ml PBS buffer was injected through the femoral vein, allowing the dye to stain the nonischemic portion of the heart and determine the ischemic area-at-risk (IAR). The entire heart was excised, rinsed of excess dye with cold saline solution, and weighed. ^{99m}Tc activity in the heart was measured by a CRC-15W Dose Calibrator/Well Counter (Capintec, Ramsey, NJ). Great vessels, atria, and right ventricles of the heart were removed. The left ventricle was sectioned into 4 or 5 transverse slices, and both sides of all slices were photographed using a digital camera. Triphenyltetrazolium chloride (TTC) staining was used to identify the infarct area. The tissue slices were incubated in a 1% TTC PBS-buffered solution (pH = 7.4) at 37°C for 20 minutes and subsequently fixed in 10% PBS-buffered formalin overnight at 2-8°C. Photographs were taken again of both sides of each TTC-stained tissue slice using the digital camera. The area unstained by Evans blue, as well as the TTC-negative area (white or pale), was quantitatively analyzed using the software of SigmaScan (SPSS Science, Chicago, IL) in trace-measurement mode. Infarct sizes were calculated as a percentage of total LV mass (% LV) and then normalized by IAR (% IAR).

Nonischemic viable (Evans blue and TTC positive) and ischemic nonviable (Evans blue and TTC negative) segments were dissected from all tissue slices. Theoretically, the remaining tissues would be ischemic viable. However, TTC staining is not precise

enough to delineate myocyte injury in detail. Focal irreversible micro-necroses might be neglected in the tissue with TTC-positive staining. It is difficult to dissect a small piece of tissue from the rat heart into TTC-positive and TTC-negative segments ascertainably. After the nonischemic viable and ischemic nonviable tissues were separated, the remaining tissue segments were characterized as mixed-viability tissues in this study. The dissected tissue samples were weighed and gamma-counted by the CRC-15W Calibrator/Well Counter. The ratios of the infarcted tissue and IAR (infarcted and mixed-viability tissues) to remote nonischemic viable myocardium were calculated, respectively.

Estimation of Hot-Spot Size on FastSPECT Imaging

The hot-spot size was estimated from each transverse slice of 120-minute FastSPECT images according to the total number of pixels defined by AMIDE 0.8.15.1 2-D isocontour ROIs analysis over the hot-spot. The 2-D isocontour ROIs were defined so that they encompassed all neighboring values above 55 percentage of the maximum threshold value in the myocardium. After acquiring the number of pixels of the hot spot on each transverse slice, the total number of pixels in all slices with hot spots were calculated and defined as the size of the infarct in the whole heart. The hot-spot sizes on 120-minute images were determined in pixels for all of the animals in the 4 groups.

Data Analysis

All results were expressed as mean \pm S.E.M. The significance of the quantitative variables was assessed using one-way or two-way NOVA with subsequent Student-Newman-Keuls post-hoc pairwise tests for comparisons between groups. Comparisons between two variables within a group were made by two-way NOVA. Probability values less than 0.05 were considered significant. The correlation between GLA hot spots and infarct size as measured by TTC staining was assessed by linear regression analysis.

Ethics

All experiments were performed in accordance with the Principles of Laboratory Animal Care from the National Institutes of Health (NIH Publication 85-23, revised 1985) and were approved by the Institutional Animal Care and Use Committee (IACUC) at the University of Arizona.

RESULTS

FastSPECT Images of Myocardium with Ischemia-Reperfusion

Cardiac blood-pool activity was visualized initially within 1-2 minutes after GLA injection. The wall of the left ventricle was then partly visualized in the stenosis zone of the LCA-supplied area, which exhibited a hot spot (increased GLA uptake). The hot spot was unequivocally localized within 10-30 minutes after intravenous administration. Two hours post-injection, the hot spot could be well visualized in all tomographic image planes. Similar hot spots were detected in all rat hearts with ischemia-reperfusion imaged with GLA. The hot spots were localized on the anterior wall, lateral wall, and apex of the

left ventricles. As shown in Figure 1, gross hot-spot sizes among the hearts could be compared visually on the 3-D reconstructed FastSPECT data set and tomographic slices. The rat heart, which received IPC treatment followed by ischemia-reperfusion, showed a smaller hot spot on the anterior lateral wall of the left ventricle compared to the larger hot spot in the heart without IPC treatment.

Quantitative Analysis of GLA Imaging

Myocardial TACs were generated using computerized ROI analysis with background, decay, acquisition time, and injected-dose correction. Raw TACs in each group are shown in Figure 2. The difference observed at each point in time from 5 minutes to 120 minutes between the LCA hot spot and normal zone was significant in the Control and SPT groups ($P < 0.05$), respectively. In the IPC and Vehicle groups, the difference between the LCA hot spot and normal zone started from 10 and 15 minutes.

Based on the appearances of the TACs, GLA exhibited slower washout from the LCA hot spot than the normal myocardial zone. By normalizing the radioactivity at each time point to the initial peak activity at 1 minute post-injection, the fractional retention (%) of GLA from the hot spot was significantly greater than that from the remote viable zone in all hearts. Because the first 1-minute image is composed mainly of blood-pool activity, the rapid washout from the normal zone shown on the TACs might represent mostly rapid blood pool clearance. Accordingly, the radioactivity at each time point was furthermore normalized by the activity at 5 minutes to calculate the percentage of radioactive washout

and retention. As shown in Figure 3, the fractional retention (% 5-minute peak) at the conclusion of imaging was still significantly higher in the hot spot than in the normal zone in all hearts (33.8 ± 2.6 vs. 14.5 ± 1.0 in IPC, $P < 0.05$; 63.1 ± 5.3 vs. 21.2 ± 2.4 in Control, $P < 0.05$; 54.8 ± 4.8 vs. 18.6 ± 1.7 in SPT, $P < 0.05$; 35.7 ± 9.2 vs. 15.3 ± 0.9 in Vehicle, $P < 0.05$). In particular, the hot-spot retention in the IPC group was similar to the Vehicle group but significantly lower than that in the Control and SPT groups ($P < 0.05$). The increased hot-spot retention in the SPT group was as high as in the Control group. The hot-spot retention in the Vehicle group was significantly lower than that in the Control and SPT groups ($P < 0.05$).

Figure 4 shows that the ratios of the hot-spot to normal myocardial activity increased with time following GLA administration in all hearts. In the Control group, the ratio was significantly higher than that in the IPC group beginning at 60 minutes and also significantly higher than that in the Vehicle group beginning at 75 minutes, but it was not different from the SPT group at any time point. The difference between the SPT group and the Vehicle group was significant. The final ratio was 3.6 ± 0.3 in the IPC group, 2.6 ± 0.6 in the Vehicle group, 5.2 ± 0.7 in the Control group, and 5.4 ± 0.3 in the SPT group.

Measurements of Myocardial IAR, Infarct, and Hot-Spot

The measurements of myocardial IAR, infarct, and hot spot are shown in Table 1. IAR did not differ significantly among experimental groups. Normalized by IAR, the infarct size (% IAR) in the Control and SPT groups was significantly larger than that in the IPC

and Vehicle groups, respectively. No significant difference in infarct size was found between either the hearts treated with IPC versus carrier vehicle or non-IPC Control versus SPT blockade. Relative to the Control group, there was a significant decrease in the size of hot-spot in the IPC group (44.2%) and Vehicle group (53.4%), but not in the SPT group.

The hot-spot sizes on FastSPECT images matched consistently with the unstained areas on TTC staining. There was a significant correlation between the TTC infarct measurements and GLA FastSPECT imaging ($r^2 = 0.775$, $P < 0.001$).

Distribution of GLA in the Hearts with Ischemia-Reperfusion

The whole heart radioactivity (%ID/gm) in the IPC (0.15 ± 0.03) and Vehicle (0.14 ± 0.02) groups was significantly lower than in the Control group (0.35 ± 0.04 , $P < 0.05$), as well as in the SPT group (0.31 ± 0.06 , $P < 0.05$), respectively. No statistical difference in the whole heart radioactivity between the IPC group versus the Vehicle group, as well as the Control group versus the SPT group, was found ($P > 0.05$). Table 2 shows the *ex vivo* gamma-counting results in dissected left ventricular myocardium. The area with negative TTC staining was considered as infarct tissue. In terms of the ratio of infarct/non-ischemic viable myocardium, the Control and SPT groups demonstrated a higher trend than the IPC and Vehicle groups, but this did not reach statistical significance. The distribution of GLA in the IAR, including infarct zone and mixed-viability zone, was significantly higher than that in the remote viable tissues. Specifically, the ratio of

IAR/non-ischemic viable myocardium in the Control group was higher than that in the IPC and Vehicle groups, but not in the SPT group. As expected, the difference between the SPT group and Vehicle group was significant.

DISCUSSION

Ischemic heart disease is the single leading cause of death in the United States, accounting for 1 of every 5 deaths. It is also the leading cause of congestive heart failure. Reperfusion is regarded as the primary means of salvaging myocardium in patients with evolving infarction. However, even after blood flow is restored, reperfusion injury with myocyte death may occur after a critical period of coronary occlusion [25, 26]. A variety of therapeutic strategies to prevent myocardial ischemia-reperfusion injury are being developed, but prospective trials in human subjects require large numbers of patients over durations. Currently, most existing cardioprotective research data are based on animal heart models. A noninvasive approach to assess *in vivo* pathophysiological progression in the animal models can bridge the knowledge gap in clinical translation of experimental interventions. In this present study, we were seeking to demonstrate the concept of applying stationary SPECT imaging techniques for noninvasive assessment of cardioprotection.

The time course of IPC protection consists of an initial early phase (2-3 hours) and second late phase (12-24 hours) [27]. The early phase is an immediate response caused by activation of membrane receptors and downstream kinases. The late phase is a

sustained window of protection that lasts at least 72 hours and requires synthesis of new proteins following genetic reprogramming of myocytes. The early- and late-phase cardioprotection may share certain triggers or mediators. Identified triggers to initiate ischemic preconditioning include adenosine, bradykinin, and catecholamines [28].

Adenosine has been proposed to be an important mediator of IPC because it has the potential to exert cardioprotection during all 3 windows of cardioprotection, including preconditioning, ischemia, and reperfusion [29]. Adenosine mediates its cardioprotection via a cardiac potassium-activated ATP (KATP) channel-linked mechanism [28, 30]. Although there are still controversies on how adenosine receptors (A_1 , A_{2A} , A_{2B} , and A_3) mediate the cardioprotection, it is generally accepted that the A_1 adenosine receptor is the primary receptor. Activation of the adenosine A_1 receptor plays a major role in most animal species tested, including rabbits, dogs, pigs, and humans. In rat hearts, adenosine involvement in preconditioning has been positively reported in several isolated global ischemia models and intact regional ischemia models. However, the duration of preconditioning and endpoints to assess myocardial damage in the various studies have produced conflicting results regarding the involvement of adenosine in rat hearts [31].

In the present study, the role of IPC in cardioprotection via adenosine receptor activation was well demonstrated in rat heart models. Because of the higher threshold for producing IPC, we chose a slightly longer protocol of 5 cycles of 4 minutes of coronary artery occlusion. A significant tolerance to myocardial ischemia-reperfusion injury was induced

with the IPC protocol. Ischemic-reperfused treatments in the two models with and without IPC produced an average infarct size (% IAR) of 21.0 ± 2.0 and 48.2 ± 6.3 with significant difference.

In terms of adenosine receptor blockade, we adopted a protocol similar to that reported in an isolated rat heart model by de Jonge et al. [21]. SPT was administered by continuous infusion 2 minutes before and during subsequent 30-minute ischemia and 30-minute reperfusion before GLA administration. As a result, SPT attenuated the benefits of IPC cardioprotection in the present study. This result is controversial to literature data by Ganote and others, in which it was concluded that adenosine does not involve preconditioning of rat hearts because adenosine receptor antagonists could not attenuate the cardioprotective effects of IPC [20]. The higher interstitial adenosine in rat hearts than that in other species might be one of the reasons that SPT could not abolish the cardioprotection of IPC in the literature [16, 21]. The short half-life of SPT (about 10 minutes) might be another reason for the failure to abolish the protection when it was intravenously injected as in the study reported by Li et al. [23]. Using alternative experimental protocols and administration of the adenosine agonist or antagonist, several studies in the literature have shown similar results as in this study. Headrick used a cardiac microdialysis technique and demonstrated that IPC resulted in an interstitial adenosine increase in the rat hearts [16], which required more adenosine receptor antagonist to attenuate the cardioprotective effects. Peart and Gross administered an adenosine kinase inhibitor, 5-iodotubercidin, to elevate adenosine concentrations and

found that the elevated adenosine concentrations might activate adenosine receptors and lead to pronounced cardioprotection in an open-chest rat heart model with infarction [32].

GLA is a specific necrotic marker in the very early stages of myocyte injury, but it is not an apoptotic marker [33]. The uptake of GLA is associated with disruption of the myocyte and nuclear membranes, allowing free intracellular diffusion and electrochemical binding of the negatively charged glucarate complex to positively charged histones. This uptake mechanism is driven by the avidity of glucarate to the nuclear protein, mitochondrial, and cytoplasmic proteins with a positive charge.

In the current study, the cardioprotection via the IPC pathway was assessed noninvasively by following observations relating to GLA necrosis-targeting properties. First, a smaller size of GLA hot spot was found as a direct definition of the reduced injury extension by effective IPC protection in comparison with a larger hot spot on constant myocardial ischemic area-at-risk in the hearts without IPC treatment. The size of the hot spot represents a good agreement with the infarct measurements on biochemical staining. Second, a faster kinetic washout of GLA and subsequent lower radioactive retention reflect the effectiveness of IPC against ischemia-reperfusion injury. An accelerated washout of GLA from the regional ischemic-reperfused myocardium was found in the animals with IPC. The ischemic-reperfused hearts without IPC protection showed a slower radioactive washout, which resulted in a significant increase in the retention of GLA. When the cardioprotection of IPC was abolished by SPT treatment, the

GLA retention resumed to the level in the hearts with no IPC protection. Third, the intensity of GLA distribution determined by FastSPECT imaging in the ischemic-reperfused myocardium represents the severity of ischemia-reperfusion injury, which can be evaluated by calculating the ratio of hot spot to normal zone radioactivity *in vivo*. The ratios in the hearts with IPC treatment tend towards a plateau about 1 hour after radiotracer injection. The ratios in the ischemic-reperfused hearts with no IPC protection increased progressively following GLA administration and exhibited significant difference beginning at 60 minutes post-injection in comparison with that in the hearts with IPC. This result may imply that GLA is preferentially retained in ongoing injured myocardium after onset of ischemia-reperfusion without sufficient cardioprotection. The *ex vivo* measurements of GLA distribution in the ischemic-reperfused hearts with and without IPC confirmed the *in vivo* observations regarding GLA hot-spot uptake. Although there was no statistical difference in the measured *ex vivo* radioactivity from dissected TTC-negative tissues for the Control group versus the IPC group, as well as the SPT group versus the Vehicle group, the overall radioactivity in the unprotected hearts was significantly higher than that in the IPC-protected hearts. More specifically, in terms of GLA distribution, there was a significant difference between the protected and unprotected hearts over the entire ischemic area-at-risk. Scattered myocardial infarcts or micronecroses, which were ignored by TTC staining, might contribute to the increase of GLA uptake in the ischemic area-at-risk determined by negative Evans blue and positive TTC staining.

FastSPECT is able to perform dynamic SPECT imaging for small animals such as rats and mice. A rapid sequence of 3-D images can be acquired in the rat heart model to study the kinetic washout of radiopharmaceuticals. Thus, the myocardial GLA radioactivity could be quantified, and the myocardial washout of GLA was determined effectively in the present study. Dynamic GLA FastSPECT imaging takes advantage of the high spatial and temporal resolution of modern imaging techniques and provides an ideal investigational tool to evaluate various interventional protocols, such as ischemic and pharmaceutical preconditioning. It provides investigators with a unique tool to assess myocytic injury, differentiate reversible and irreversible myocardial damage, and evaluate various cardioprotective strategies. Without sacrificing animals, myocardial injury and salvaged amounts can be determined by quantifying the size of hot spots, measuring the accumulation of GLA, and calculating the kinetic washout of GLA. The ongoing cardioprotection can be examined in the early or delayed phase, depending on the experimental procedures.

Although an advanced stationary SPECT system was applied, there were several limitations in this study partly because of the small rat heart and lack of techniques. The low level of GLA accumulation in normal myocardium makes it difficult to calculate the percent of infarct over the whole left ventricle in hearts with small infarcts. Instead of calculating the percent infarct of the left ventricle, we quantified the number of pixels of the hot spot on the tomographic images of GLA. One pixel equals 1×1 mm in the reconstructed images in our SPECT system; the size of the hot spot could be estimated. It

is also challenging to control the errors in the resulting hot-spot quantification because it is difficult to obtain “ground truth” from which to find the boundary and segment of the image into infarct and non-infarct regions. Because there is essentially little or no GLA uptake in normal myocardium, the ROI location must be carefully selected to avoid the ROI on the early time-point images not overlapping into the ventricular chamber and being contaminated by the blood pool. Small changes in the ROI location could result in significant differences in the radioactive ratios of ischemic zone to normal zone. In the current study, we applied tomographic blood-pool images to ensure the ROI establishment off the left ventricular cavity. The quantification of radioactive hot spots in rats with smaller infarcts might be facilitated by the use of dual-isotope SPECT imaging with GLA and a perfusion tracer like ^{201}Tl . A dual-modality small-animal SPECT/CT system may be useful to identify the endocardial edges from X-ray CT by administration of contrast agents. Using the physically coregistered SPECT/CT images, the total radiotracer activity in the myocardium may be determined more accurately. We did not correct for radioactive scatter because the scatter influence from adjacent non-cardiac structures is minimal in FastSPECT. Gating SPECT imaging provides a valuable adjunct in enhancing the assessment of infarct avid imaging. However, gating imaging acquisition is impractical in FastSPECT, but is available in a new system, FastSPECT II, also built in our laboratory.

In conclusion, significant tolerance to myocardial ischemia-reperfusion injury, as assessed by biochemical assay and noninvasive infarct-avid imaging, was induced with

an ischemic preconditioning protocol in the rat model. Adenosine antagonist SPT could block the cardioprotection of ischemic preconditioning. Thus, the preconditioning cardioprotection is in direct relationship with the activation of adenosine receptors in rat hearts. ^{99m}Tc -glucarate FastSPECT imaging is not only useful in detecting early ischemia-reperfusion injury, but is valuable in evaluating the effects of cardioprotective treatments. Quantitative analysis of dynamic images with ^{99m}Tc -glucarate provides a unique tool for evaluation of cardioprotection. High-resolution imaging studies in small-animal models in cardiology permit longitudinal studies in the same animals. Such imaging studies, once validated, can yield data that will serve as biomarkers for effects of drug intervention.

Acknowledgements

The authors wish to acknowledge the technical support of Christy Barber and editorial assistance of Corrie Thies. This work was supported by NIH grant P41 EB002035. Dr. Koon Yan Pak is a shareholder in Molecular Targeting Technologies, Inc.

References

1. Liu Z, Barrett HH, Stevenson GD, Kastis GA, Bettan M, Furenlid LR, et al. High-resolution imaging with (99m)Tc-glucarate for assessing myocardial injury in rat heart models exposed to different durations of ischemia with reperfusion. *J Nucl Med* 2004; 45:1251-1259.
2. Liu Z, Kastis GA, Stevenson GD, Barrett HH, Furenlid LR, Kupinski MA, et al. Quantitative analysis of acute myocardial infarct in rat hearts with ischemia-reperfusion using a high-resolution stationary SPECT system. *J Nucl Med* 2002; 43:933-939.
3. Acton PD, Kung HF. Small animal imaging with high resolution single photon emission tomography. *Nucl Med Biol* 2003; 30:889-895.
4. Miyagawa M, Anton M, Haubner R, Simoes MV, Stadele C, Erhardt W, et al. PET of cardiac transgene expression: comparison of 2 approaches based on herpesviral thymidine kinase reporter gene. *J Nucl Med* 2004; 45:1917-1923.
5. Simoes MV, Miyagawa M, Reder S, Stadele C, Haubner R, Linke W, et al. Myocardial kinetics of reporter probe 124I-FIAU in isolated perfused rat hearts after in vivo adenoviral transfer of herpes simplex virus type 1 thymidine kinase reporter gene. *J Nucl Med* 2005; 46:98-105.
6. Johnson G, 3rd, Okada CC, Hocherman SD, Liu Z, Hart C, Khaw BA, et al. (99m)Tc-glucarate imaging for the early detection of infarct in partially reperfused canine myocardium. *Eur J Nucl Med Mol Imaging* 2006; 33:319-328.

7. Okada DR, Johnson G, Liu Z, Hocherman SD, Khaw BA, Okada RD. Early detection of infarct in reperfused canine myocardium using ^{99m}Tc -glucarate. *J Nucl Med* 2004; 45:655-664.
8. Johnson LL, Schofield L, Mastrofrancesco P, Donahay T, Farb A, Khaw BA. Technetium-99m glucarate uptake in a swine model of limited flow plus increased demand. *J Nucl Cardiol* 2000; 7:590-598.
9. Narula J, Petrov A, Pak KY, Lister BC, Khaw BA. Very early noninvasive detection of acute experimental nonreperfused myocardial infarction with ^{99m}Tc -labeled glucarate. *Circulation* 1997; 95:1577-1584.
10. Khaw BA, Nakazawa A, O'Donnell SM, Pak KY, Narula J. Avidity of technetium-99m glucarate for the necrotic myocardium: in vivo and in vitro assessment. *J Nucl Cardiol* 1997; 4:283-290.
11. Orlandi C, Crane PD, Edwards DS, Platts SH, Bernard L, Lazewatsky J, et al. Early scintigraphic detection of experimental myocardial infarction in dogs with technetium-99m-glucaric acid. *J Nucl Med* 1991; 32:263-268.
12. Murry CE, Jennings RB, Reimer KA. Preconditioning with ischemia: a delay of lethal cell injury in ischemic myocardium. *Circulation* 1986; 74:1124-1136.
13. Cohen MV, Liu GS, Downey JM. Preconditioning causes improved wall motion as well as smaller infarcts after transient coronary occlusion in rabbits. *Circulation* 1991; 84:341-349.
14. Schott RJ, Rohmann S, Braun ER, Schaper W. Ischemic preconditioning reduces infarct size in swine myocardium. *Circ Res* 1990; 66:1133-1142.

15. Wannenburg T, de Tombe PP, Little WC. Effect of adenosine on contractile state and oxygen consumption in isolated rat hearts. *Am J Physiol* 1994; 267:H1429-1436.
16. Headrick JP. Ischemic preconditioning: bioenergetic and metabolic changes and the role of endogenous adenosine. *J Mol Cell Cardiol* 1996; 28:1227-1240.
17. Ballard-Croft C, Kristo G, Yoshimura Y, Reid E, Keith BJ, Mentzer RM, Jr., et al. Acute adenosine preconditioning is mediated by p38 MAPK activation in discrete subcellular compartments. *Am J Physiol Heart Circ Physiol* 2005; 288:H1359-1366.
18. Liu Y, Downey JM. Ischemic preconditioning protects against infarction in rat heart. *Am J Physiol* 1992; 263:H1107-1112.
19. Li Y, Kloner RA. Adenosine deaminase inhibition is not cardioprotective in the rat. *Am Heart J* 1993; 126:1293-1298.
20. Ganote CE, Armstrong SC. Adenosine and preconditioning in the rat heart. *Cardiovasc Res* 2000; 45:134-140.
21. de Jonge R, de Jong JW, Giacometti D, Bradamante S. Role of adenosine and glycogen in ischemic preconditioning of rat hearts. *Eur J Pharmacol* 2001; 414:55-62.
22. Liem DA, van den Doel MA, de Zeeuw S, Verdouw PD, Duncker DJ. Role of adenosine in ischemic preconditioning in rats depends critically on the duration of the stimulus and involves both A(1) and A(3) receptors. *Cardiovasc Res* 2001; 51:701-708.
23. Li Y, Kloner RA. The cardioprotective effects of ischemic "preconditioning" are not mediated by adenosine receptors in rat hearts. *Circulation* 1993; 87:1642-1648.

24. Rowe RK, Aarsvold JN, Barrett HH, Chen JC, Klein WP, Moore BA, et al. A stationary hemispherical SPECT imager for three-dimensional brain imaging. *J Nucl Med* 1993; 34:474-480.
25. Verma S, Fedak PW, Weisel RD, Butany J, Rao V, Maitland A, et al. Fundamentals of reperfusion injury for the clinical cardiologist. *Circulation* 2002; 105:2332-2336.
26. Claeys MJ, Bosmans J, Veenstra L, Jorens P, De Raedt H, Vrints CJ. Determinants and prognostic implications of persistent ST-segment elevation after primary angioplasty for acute myocardial infarction: importance of microvascular reperfusion injury on clinical outcome. *Circulation* 1999; 99:1972-1977.
27. Guo Y, Wu WJ, Qiu Y, Tang XL, Yang Z, Bolli R. Demonstration of an early and a late phase of ischemic preconditioning in mice. *Am J Physiol* 1998; 275:H1375-1387.
28. Cohen MV, Baines CP, Downey JM. Ischemic preconditioning: from adenosine receptor to KATP channel. *Annu Rev Physiol* 2000; 62:79-109.
29. Vinten-Johansen J, Zhao ZQ, Corvera JS, Morris CD, Budde JM, Thourani VH, et al. Adenosine in myocardial protection in on-pump and off-pump cardiac surgery. *Ann Thorac Surg* 2003; 75:S691-699.
30. Headrick JP, Hack B, Ashton KJ. Acute adenosinergic cardioprotection in ischemic-reperfused hearts. *Am J Physiol Heart Circ Physiol* 2003; 285:H1797-1818.
31. Vasara E, Katharou I, Lazou A. Myocardial adenosine does not correlate with the protection mediated by ischaemic or pharmacological preconditioning in rat heart. *Clin Exp Pharmacol Physiol* 2003; 30:350-356.

32. Peart JN, Gross GJ. Cardioprotection following adenosine kinase inhibition in rat hearts. *Basic Res Cardiol* 2005; 100:328-336.
33. Khaw BA, Silva JD, Petrov A, Hartner W. Indium 111 antimyosin and Tc-99m glucaric acid for noninvasive identification of oncotic and apoptotic myocardial necrosis. *J Nucl Cardiol* 2002; 9:471-481.

Legends for illustrations

Figure 1:

A visual comparison of GLA hot-spot accumulations in two representative ischemic-reperfused rat hearts treated with the protocol of IPC in the IPC group (left panel) and without cardioprotection in the Control group (right panel) 120 minutes post-injection. The wall of the left ventricle was partly visualized on 3-D representation of a reconstructed FastSPECT data set of the left ventricle (A and E). The hot spots localized in the lateral wall, anterior wall, and apex of the left ventricles. Larger hot spots were demonstrated on tomographic transaxial, coronal, and sagittal slices (B-D) in the Control heart without IPC protection than that in the IPC-protected heart (F-H).

Figure 2:

GLA kinetic time-activity curves from normal and ischemic-reperfused areas in the hearts of all 4 groups. The curves were corrected by radioactive decay, acquisition time, and injected dose. There was a significant difference between the LCA hot spot and normal zone at each time point from 5 minutes to 120 minutes in the Control and SPT groups. The difference was significant from 10 minutes to 120 minutes in the IPC group, and 15 minutes to 120 minutes in the Vehicle group ($P < 0.05$).

Figure 3:

The fractional retention (%) of GLA from the hot-spot and remote viable zone calculated by normalizing the radioactivity at the end of the imaging session to the initial 1-minute

and 5-minute peak activity on FastSPECT images. The retention from the hot-spot was significantly greater than that from the remote viable zone in all hearts. # = $P < 0.05$ compared to the hot spot in the Control group at 1-minute as initial peak; & = $P < 0.05$ compared to the normal zone in the Control group at 5-minute as initial peak; * = $P < 0.05$ compared to the hot spot in the Control group at 5-minute as initial peak; @ = $P < 0.05$ compared to the hot spot in the Vehicle group.

Figure 4:

Ratios of the hot spot to viable myocardial GLA activity over time from the hearts of all 4 groups. * = $P < 0.05$ compared to the Control group.

TABLE 1. Measurements of myocardial ischemic area at risk (IAR), infarct and GLA hot spot

	IAR (%LV)	Infarct (%LV)	Infarct (%IAR)	Hot spot (Pixels)
IPC (n = 6)	49.4±3.9	10.1±0.6*	21.0±2.0*	624.5±74.1*
Control (n = 7)	48.8±2.9	23.8±3.7	48.2±6.3	1118.4±102.6
SPT (n = 6)	46.2±4.6	18.9±2.9†	41.7±6.3†	1043.9±185.0†
Vehicle (n = 5)	47.7±5.2	8.4±1.7*	19.1±4.6*	624.5±74.1*

mean ± SEM. * = $P < 0.05$ compared to Control; † = $P < 0.05$ compared to Vehicle.

TABLE 2. Ex vivo gamma counting results (Ratios)

	Infarct/NIV	MV/NIV	IAR/NIV
IPC (n = 6)	6.19±1.45	1.66±0.19*	3.04±0.41*
Control (n = 7)	9.62±1.32	3.36±0.53	7.37±0.98†
SPT (n = 6)	10.45±1.92	4.87±0.86*†	7.37±1.40†
Vehicle (n = 5)	6.56±1.11	2.38±0.22	3.36±0.48*

mean ± SEM. * = $P < 0.05$ compared to Control; † = $P < 0.05$ compared to Vehicle. MV: mixed-viability; NIV: non-ischemic viable; IAR: ischemic area at risk (Infarct and mixed-viability).

Figure 1
[Click here to download high resolution image](#)

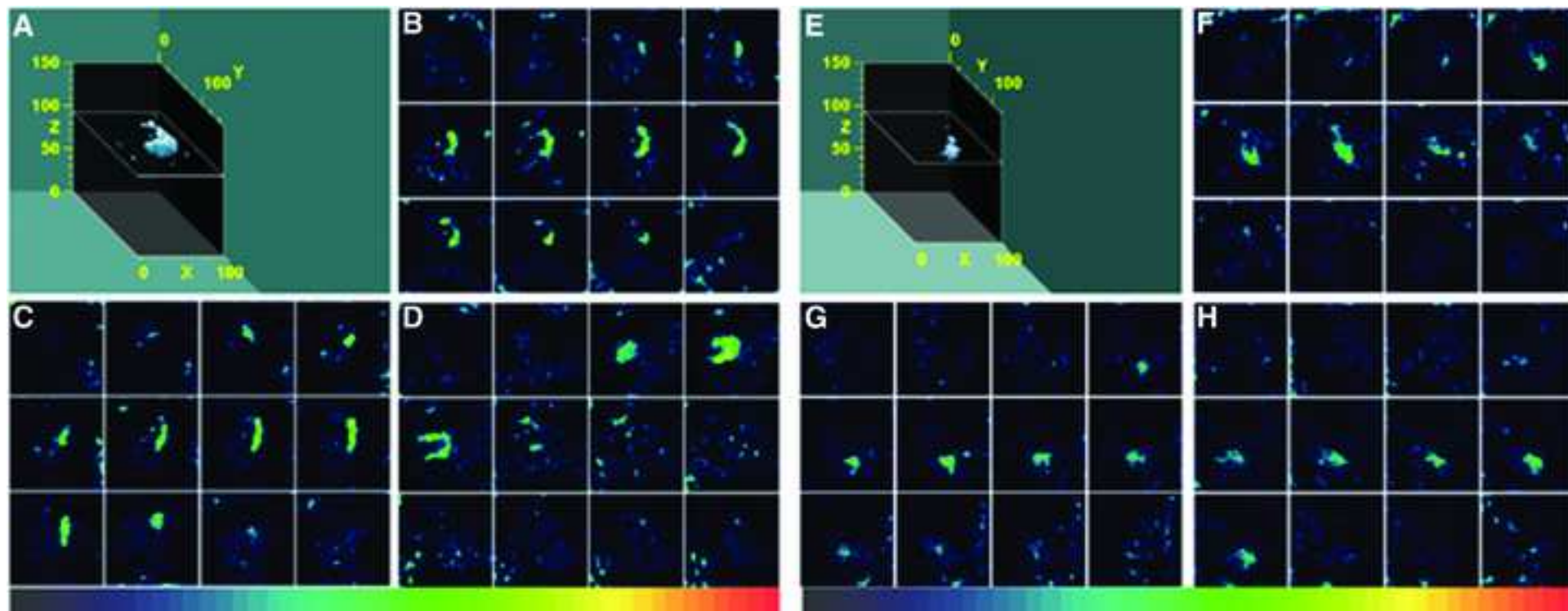


Figure 2
[Click here to download high resolution image](#)

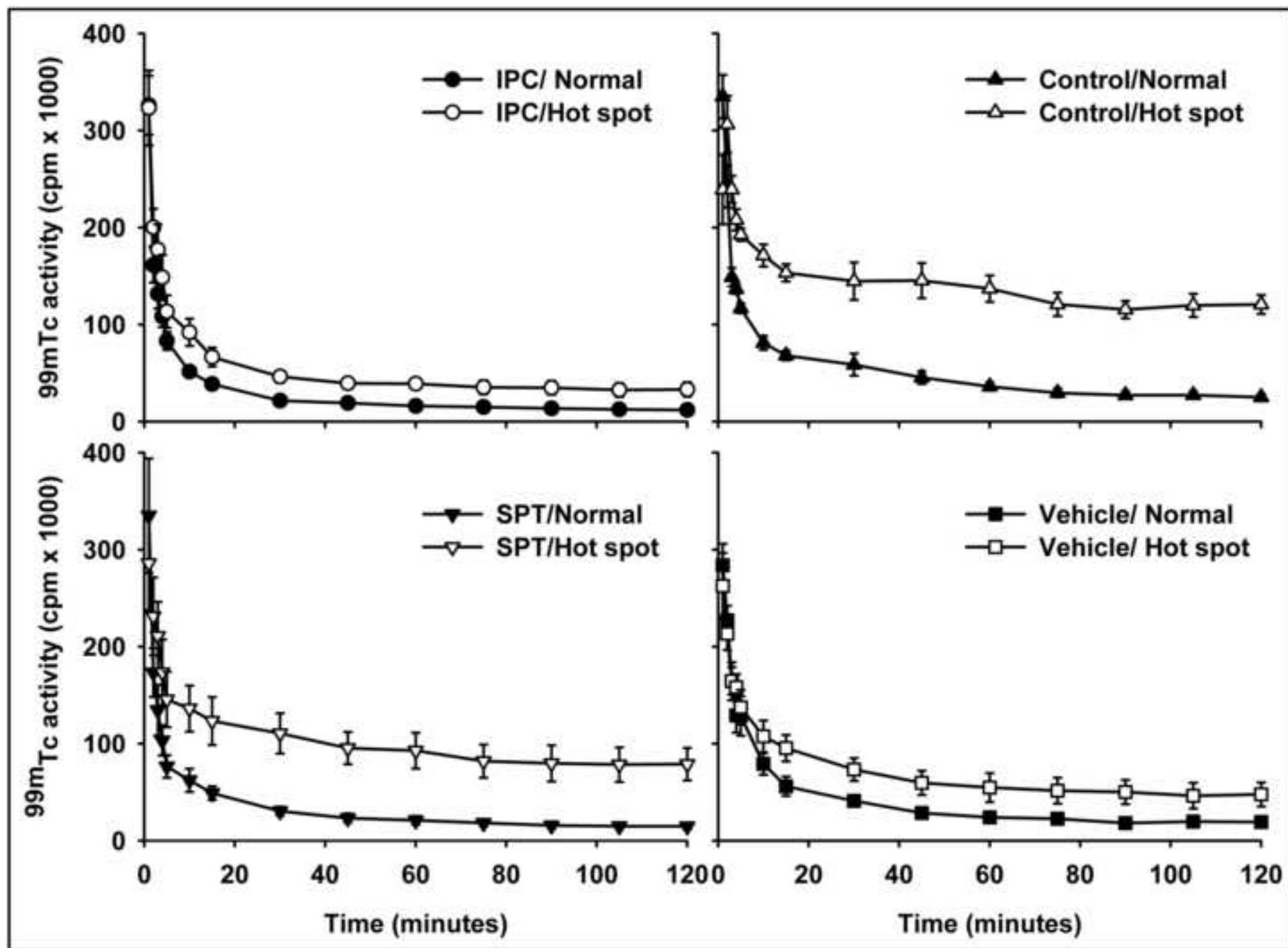


Figure 3
[Click here to download high resolution image](#)

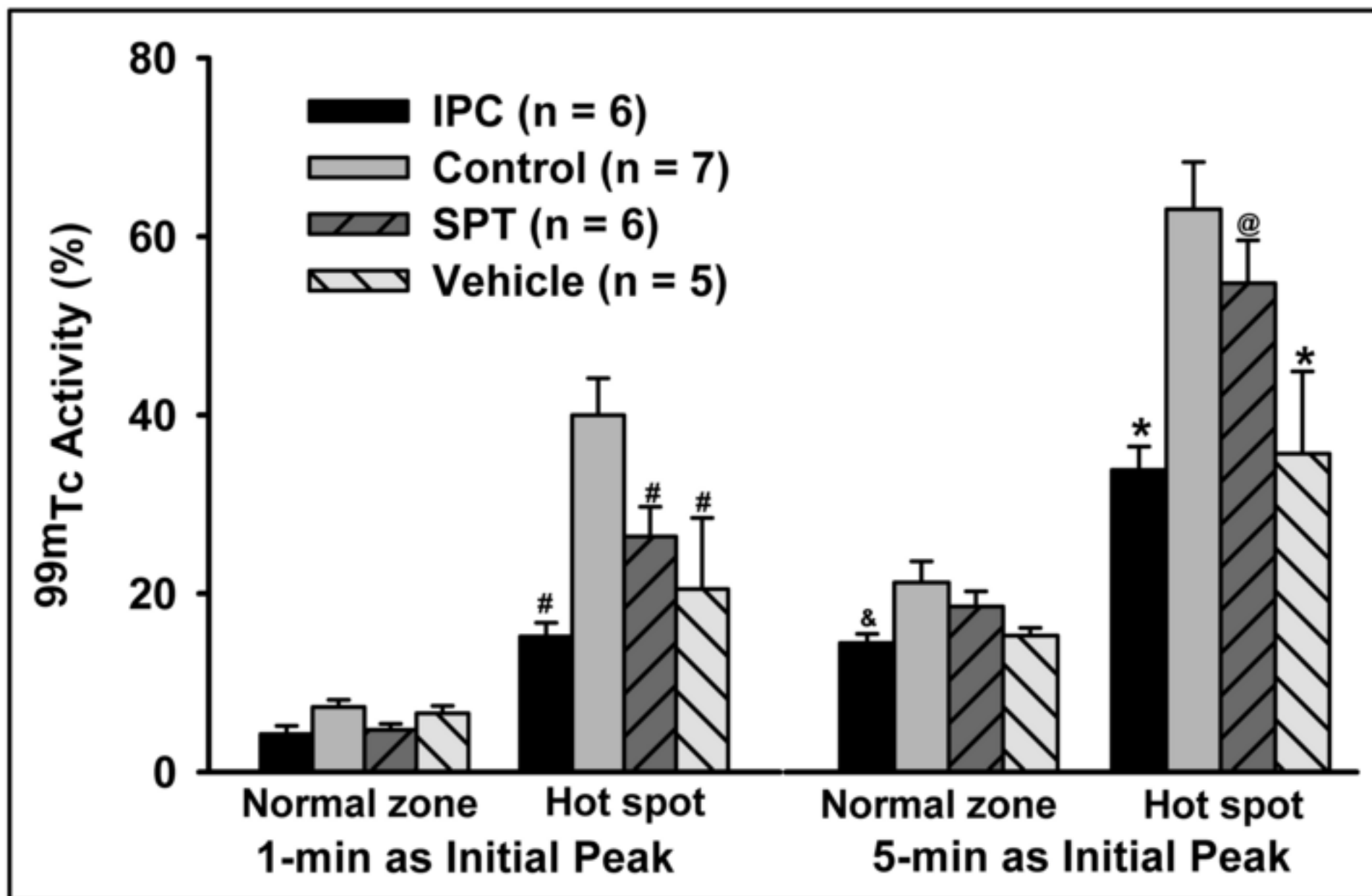
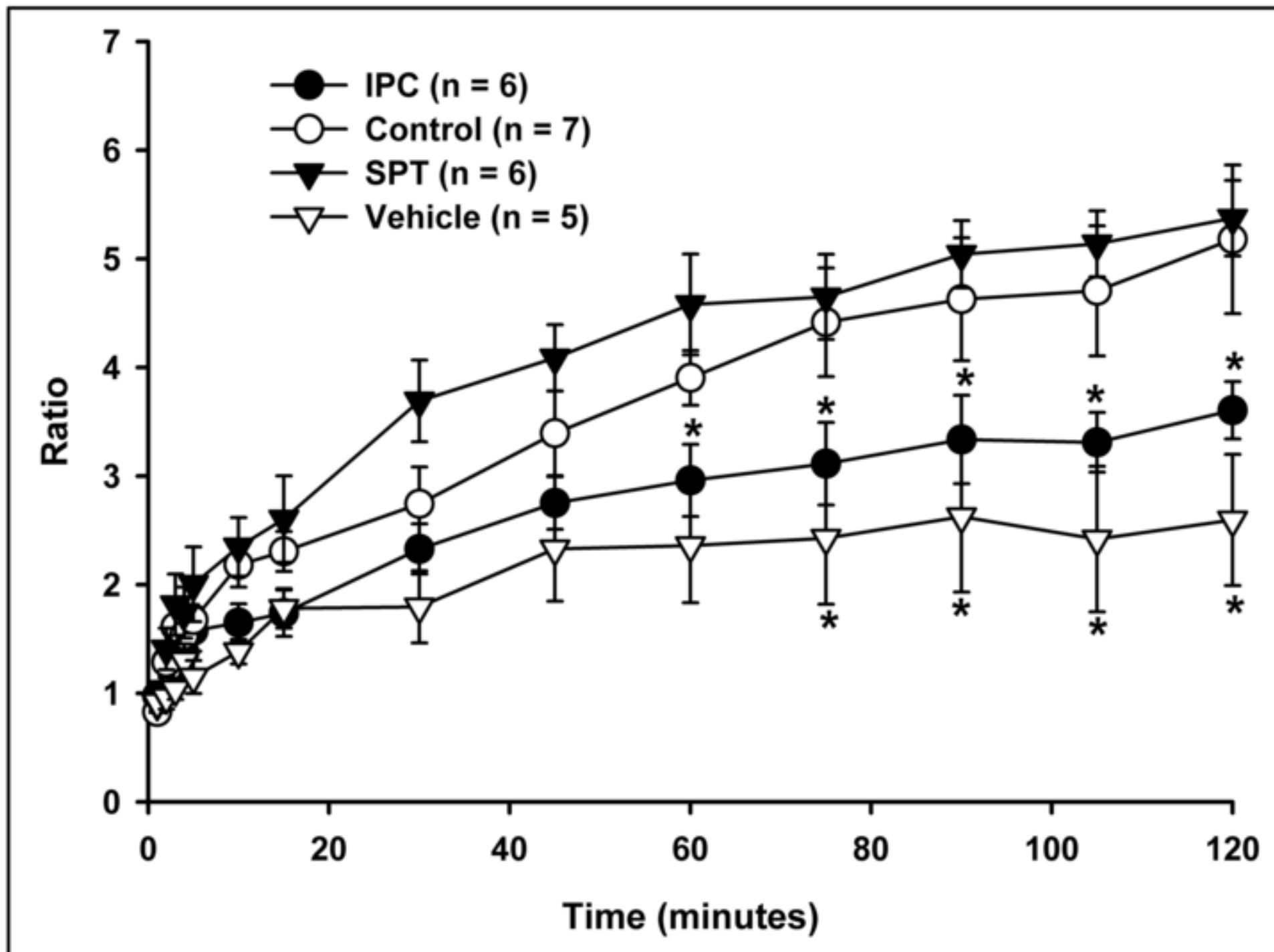


Figure 4
[Click here to download high resolution image](#)



September 24, 2007

Dear Reviewer:

Thank you for your comments regarding our manuscript. Enclosed please find the revised manuscript. All issues raised by both reviewers have been addressed. The original Figure 1 has been removed and figure orders have been re-numbered. The authors believe that the manuscript should now be acceptable for publication pending your review. The authors wish to thank you for suggesting changes, which resulted in strengthening of the manuscript.

The following are our responses to your Specific Comments:

1. Figure 1 shows representative dynamic images in a control rat. But, similar figures appeared in their previous paper (JNM,2004, 45,1251-1259), and it is not the focus of this paper. I recommend to remove it.

Figure 1 has been removed.

2. Please provide scale bars in figure 2 indicating an absolute value (%ID/g), to make clear the differences of tracer intensity among the groups. Fused image with additional perfusion study would be better to see the localization of tracer uptake. Reference image to delineate the heart is required for hot spot images.

Currently, we have technical difficulties to determine the correlation between the radioactive counts per voxel detected by FastSPECT imaging and the absolute tissue radioactive value (%ID/g). A complicated calibration measurement is required. The ex vivo data of whole heart radioactivity (%ID/gm) in 4 groups were determined and reported in the paper.

We agree that a fused image with additional perfusion study would be ideal to localize the tracer uptake in the myocardium. However, we did not perform additional perfuse imaging in the ischemic-reperfused hearts in the present study. FastSPECT is able to perform fast dynamic SPECT imaging for small animals. We took advantages of the FastSPECT and collected the early blood-pool image (which we're deleting from Fig. 1) to generate a cardiac outline. The endocardial edges from tomographic 1-minute cardiac blood-pool images were coregistered with 120-minute images to localize the hot spot accumulation of ^{99m}Tc in the left ventricular walls. In a new version of FastSPECT, FastSPECT II, which is a dual-modality small-animal SPECT/CT system, we will be able to identify the endocardial edges from X-ray CT by administration of contrast agents.

Again, thank you for your time and suggestions.

Best regards,

Authors

To Reviewer #1

September 24, 2007

Dear Reviewer:

Thank you for your comments regarding our manuscript. Enclosed please find the revised manuscript. All issues raised by both reviewers have been addressed. The original Figure 1 has been removed and figure orders have been re-numbered. The authors believe that the manuscript should now be acceptable for publication pending your review. The authors wish to thank you for suggesting changes, which resulted in strengthening of the manuscript.

The following are our responses to your Specific Comments:

1. Scanner specification. Although scans are presented in Figure 1 and this gives the reader a feel for the spatial resolution of the scanner, it would be helpful if the resolution could be stated in the text.

The spatial resolution of the system is 1.0 mm, which has been stated in the manuscript as you suggested.

2. Lesion size. In the section on estimation of hot-spot size it is stated that this was quantified by summing all the pixels. It is not made clear here what determined whether or not a pixel was included in the count. What threshold was adopted and how reproducible were the measurements? Some of the limitations are discussed at the end of the paper, but the authors should clarify how the measurements were made.

As you suggested, a paragraph “**Estimation of Hot-Spot Size on FastSPECT Imaging**” has been rewritten to clarify how the measurements were made. In brief, the lesion size was estimated from each transverse slice of 120-minute FastSPECT images according to the number of pixels defined by a computerized ROI analysis around the hot-spot. Because it is difficult to obtain “ground truth” from which to find the boundary of the hot spot, we determined the hot spot size or volume by 2-D isocontour ROIs analysis over the hot-spot using AMIDE 0.8.15.1 software. The reconstructed images were displayed with the maximum threshold 30-35% and minimum threshold 0%. A 2-D isocontour ROI was derived so that it encompasses all neighboring values above 55 percentage of the maximum threshold in the myocardium. This measurement is highly reproducible.

Again, thank you for your time and suggestions.

Best regards,

Authors

To Reviewer #2

Nuclear Medicine Communications

Authorship Responsibility, Financial Disclosure, and Copyright Transfer

Manuscript Title: 99mTc-glucarate SPECT imaging of rat heart(the "Work") MS number:

Corresponding Author: Zhonglin Liu

Mailing Address and Telephone/Fax Numbers:P.O. Box 245067, Tucson, AZ 85724-5067, USA

Phone 520-626-4248; Fax 520-626-2892

Each author must read and sign the following statements; if necessary, photocopy this document and distribute to all coauthors for their original ink signatures. Completed forms should be submitted to the Editorial Office with the Work or returned to: **Angela Kitt, Production Editor, Lippincott Williams & Wilkins, 250 Waterloo Road, London SE1 8RD, UK.**

CONDITIONS OF SUBMISSION

RETAINED RIGHTS: Except for copyright, other proprietary rights related to the Work (e.g., patent or other rights to any process or procedure) shall be retained by the authors. To reproduce any text, figures, tables, or illustrations from this Work in future works of their own, the authors must obtain written permission from Lippincott Williams & Wilkins (LWW); such permission cannot be unreasonably withheld by LWW.

ORIGINALITY: Each author warrants that his or her submission to the Work is original and that he or she has full power to enter into this agreement. Neither this Work nor a similar work has been published nor shall be submitted for publication elsewhere while under consideration by this Publication.

AUTHORSHIP RESPONSIBILITY: Each author warrants that he or she has participated sufficiently in the intellectual content, the analysis of data, if applicable, and the writing of the Work to take public responsibility for it. Each has reviewed the final version of the Work, believes it represents valid work, and approves it for publication. Moreover, should the editors of the Publication request the data upon which the work is based, they shall produce it.

DISCLAIMER: Each author warrants that this Work shall not violate any trademark registrations or the right of privacy of any person, contains no libellous, obscene, or other unlawful matter, and does not infringe upon the statutory or common law copyright or any other right of any person or party. If excerpts (text, figures, tables, or illustrations) from copyrighted works are included, a written release will be secured by the authors prior to submission, and credit to the original publication will be properly acknowledged. Each author further warrants that he or she has obtained, prior to submission, written releases from patients whose names or photographs are submitted as part of the Work. Should LWW request copies of such written releases, authors shall provide them to LWW in a timely manner.

TRANSFER OF COPYRIGHT

AUTHORS' OWN WORK: In consideration of LWW's publication of the Work, the authors hereby transfer, assign, and otherwise convey all copyright ownership worldwide, in all languages, and in all forms of media now or hereafter known, including electronic media such as CD-ROM, Internet, and Intranet, to LWW. If LWW should decide for any reason not to publish an author's submission to the Work, LWW shall give prompt notice of its decision to the corresponding author, this agreement shall terminate, and neither the author nor LWW shall be under any further liability or obligation. Each author grants LWW the rights to use his or her name and biographical data (including professional affiliation) in the Work and in its or the Publication's promotion.

WORK MADE FOR HIRE: If this work has been commissioned by another person or organization, or if it has been written as part of the duties of an employee, an authorized representative of the commissioning organization or employer must also sign this form stating his or her title in the organization.

GOVERNMENT EMPLOYEES: If this submission to the Work has been written in the course of any author's employment by the United States Government, check the "Government" box at the end of this form. A work prepared by a government employee as part of his or her official duties is called a "work of the U.S. Government" and is not subject to copyright. If it is not prepared as part of the employee's official duties, it may be subject to copyright.

FINANCIAL DISCLOSURE: Each author warrants that he or she has no commercial associations (e.g., consultancies, stock ownership, equity interest, patent/licensing arrangements, etc.) that might pose a conflict of interest in connection with the submitted article, except as disclosed on a separate attachment. All funding sources supporting the Work and all institutional or corporate affiliations of the authors are acknowledged in a footnote in the Work.

INSTITUTIONAL REVIEW BOARD/ANIMAL CARE COMMITTEE APPROVAL: Each author warrants that his or her institution has approved the protocol for any investigation involving humans or animals and that all experimentation was conducted in conformity with ethical and humane principles of research.

	Zhonglin Liu	07-17-2007
Signature	Printed Name	Date
<input checked="" type="checkbox"/> Author's Own Work	<input type="checkbox"/> Work for Hire <input type="checkbox"/> Government	<input checked="" type="checkbox"/> Financial Disclosure Attached
	Harrison Barrett, Gail Stevenson	07-18-2007
Signature	Printed Name	Date
<input checked="" type="checkbox"/> Author's Own Work	<input type="checkbox"/> Work for Hire <input type="checkbox"/> Government	<input checked="" type="checkbox"/> Financial Disclosure Attached
	Lars Furenlid James Woolfenen	07-18-2007
Signature	Printed Name	Date
<input checked="" type="checkbox"/> Author's Own Work	<input type="checkbox"/> Work for Hire <input type="checkbox"/> Government	<input checked="" type="checkbox"/> Financial Disclosure Attached
	Koon Yan Pak	07-18-2007
Signature	Printed Name	Date
<input type="checkbox"/> Author's Own Work	<input type="checkbox"/> Work for Hire <input type="checkbox"/> Government	<input type="checkbox"/> Financial Disclosure Attached